© 2017. Published by The Company of Biologists Ltd | Journal of Experimental Biology (2017) 220, 425-436 doi:10.1242/jeb.145615

RESEARCH ARTICLE

Ammonia excretion in the marine polychaete *Eurythoe complanata* (Annelida)

Daniel Thiel[1,*,‡], Maja Hugenschütt[1,‡], Heiko Meyer[1], Achim Paululat[1], Alex R. Quijada-Rodriguez[2], Günter Purschke[1] and Dirk Weihrauch[2,§]

ABSTRACT

Ammonia is a toxic waste product from protein metabolism and needs to be either converted into less toxic molecules or, in the case of fish and aquatic invertebrates, excreted directly as is. In contrast to fish, very little is known regarding the ammonia excretion mechanism and the participating excretory organs in marine invertebrates. In the current study, ammonia excretion in the marine burrowing polychaete *Eurythoe complanata* was investigated. As a potential site for excretion, the 100–200 µm long, 30–50 µm wide and up to 25 µm thick dentrically branched, well ventilated and vascularized branchiae (gills) were identified. In comparison to the main body, the branchiae showed considerably higher mRNA expression levels of Na^+/K^+-ATPase, V-type H^+-ATPase, cytoplasmic carbonic anhydrase (CA-2), a Rhesus-like protein, and three different ammonia transporters (AMTs). Experiments on the intact organism revealed that ammonia excretion did not occur via apical ammonia trapping, but was regulated by a basolateral localized V-type H^+-ATPase, carbonic anhydrase and intracellular cAMP levels. Interestingly, the V-type H^+-ATPase seems to play a role in ammonia retention. A 1 week exposure to 1 mmol l^{-1} NH_4Cl (HEA) did not cause a change in ammonia excretion rates, while the three branchial expressed AMTs showed a tendency to be down-regulated. This indicates a shift of function in the branchial ammonia excretion processes under these conditions.

KEY WORDS: AMTs, Gill morphology, V-ATPase, cAMP, Acid–base regulation, HEA

INTRODUCTION

Ammonia (in this study NH_3 refers to gaseous ammonia, NH_4^+ to ammonium ions, and ammonia to the sum of the two) is a toxic waste product from protein metabolism and needs to be either detoxified into less toxic molecules or rapidly excreted to avoid detrimental accumulation in the body fluids (Larsen et al., 2014). For instance, in the shrimp *Penaeus stylirostri*, elevated ammonia levels reduced the total number of immune active haemocytes (Le Moullac and Haffner, 2000), and in lobster and crayfish exposure to ammonia disrupts ionoregulatory functions (Harris et al., 1998; Young-Lai et al., 1991). For further information on toxic effects of ammonia in other animals including vertebrates, please refer to Larsen et al. (2014).

With very few exceptions, aquatic species such as teleost fish (Weihrauch et al., 2009; Wright and Wood, 2009), fully aquatic amphibians (Cragg et al., 1961; Fanelli and Goldstein, 1964; Wood et al., 1989) and virtually all aquatic invertebrates investigated so far are ammonotelic (Larsen et al., 2014; Wright, 1995), excreting the majority of their nitrogenous waste in the form of ammonia directly into the environment. Most of the ammonia is usually excreted via the gas-exchanging and ion-regulating branchiae (gills), well documented for fish and decapod crabs (Weihrauch and O'Donnell, 2015; Weihrauch et al., 2009; Wright and Wood, 2009). If classic branchiae are absent, ammonia is excreted through other appendices such as the anal papillae found in some aquatic insect larvae (Donini and O'Donnell, 2005; Weihrauch et al., 2011). In addition, the skin (epidermal tissue) plays an import role in the excretion process when appendices are absent, as reported for some amphibians such as the African clawed frog *Xenopus laevis* and the neotenous newt *Necturus maculosus* (Cruz et al., 2013; Fanelli and Goldstein, 1964), but also for leeches (Quijada-Rodriguez et al., 2015), planarians (Weihrauch et al., 2012) and nematodes (Adlimoghaddam et al., 2015).

The actual transepithelial ammonia excretion mechanism varies between tissues and species but usually involves a basolateral Na^+/K^+-ATPase (NKA), which actively transports NH_4^+ in exchange for Na^+ ions from the body fluids into the epithelial cell (Masui et al., 2002; Quijada-Rodriguez et al., 2015; Weihrauch et al., 1998), and a Rhesus-like (Rh)-protein which mediates basolateral ammonia transport (Adlimoghaddam et al., 2015; Nakada et al., 2007; Weihrauch et al., 2009). Further evidence is available suggesting that in freshwater organisms the exit of cellular ammonia occurs via apically localized Rh-proteins, a process energized by a co-localized V-type H^+-ATPase (HAT) that acidifies the apical unstirred boundary layer, thereby generating an outwardly directed partial pressure gradient for NH_3 (ΔP_{NH_3}). This process might be supported by a co-localized Na^+/H^+-exchanger (NHE). The catalytic action of the carbonic anhydrase provides protons in this system (Weihrauch et al., 2012; Wright and Wood, 2009). For pH-buffered environments such as seawater or soil, a vesicular ammonia excretion mechanism has also been proposed. Evidence suggested that in this mechanism ammonia is trapped in acidified vesicles, which are then transported along the microtubule network to the apical membrane of the epithelia cell, where NH_4^+ is excreted via exocytosis (Adlimoghaddam et al., 2015; Weihrauch et al., 2002).

Very limited information exists regarding the ammonia excretion mechanism or the actual site of excretion in marine polychaetous annelids. However, all marine polychaetes studied so far appear to be ammonotelic. For *Nereis succinea* and *Nereis virens*, an active excretion was shown which depends partially on the activity of the NKA (Mangum, 1978). The site of excretion, however, is still

[1]University of Osnabrück, Fachbereich Biologie, Department of Zoology, Osnabrück 49069, Germany. [2]University of Manitoba, Department of Biological Sciences, Winnipeg, Manitoba, Canada.
*Present address: Sars International Centre for Marine Molecular Biology, Thormøhlensgate 55, Bergen 5008, Norway
‡These authors contributed equally to this work

§Author for correspondence (Dirk.Weihrauch@ad.umanitoba.ca)

D.W., 0000-0002-3218-9093

Received 4 July 2016; Accepted 11 November 2016

Journal of Experimental Biology

Journal of Experimental Biology (2017) 220, 425-436 doi:10.1242/jeb.145615

List of symbols and abbreviations

AMT	ammonia transporter
ASW	artificial seawater
CA	carbonic anhydrase
ECM	extracellular matrix
FM	fresh mass
HAT	V-type H^+-ATPase
HEA	high environmental ammonia
NHE	Na^+/H^+-exchanger
NKA	Na^+/K^+-ATPase
PBS	phosphate-buffered saline
PBST	PBS+0.1% Tween
P_{NH_3}	partial pressure of NH_3
qPCR	quantitative PCR
Rh	Rhesus
SEM	scanning electron microscopy
TEM	transmission electron microscopy

speculative. In this context, it was suggested that besides the metanephridial system, the intensely vascularized parapodia as a whole might play a role in this process (O'Donnell, 1997).

In order to identify the site and mechanism of ammonia excretion in marine polychaetes in more detail, whole-animal transport studies, gene expression analyses and microscopy techniques were employed in the present study on a burrowing marine species, *Eurythoe complanata*, the Mexican fireworm. Our studies indicate that ventilated hand–glove-like appendices localized at the posterior base of the notopodia represent the 'branchiae' and are likely to be an important site of ammonia excretion and gas exchange. Immunohistochemistry further revealed a basolateral localization of the HAT in this tissue; unexpectedly, the enzyme seems to be involved in ammonia retention rather than in excretory processes.

MATERIALS AND METHODS

Animals

Individuals of *Eurythoe complanata* (Pallas 1766) were maintained in an established 350 l seawater tank (salinity 32‰, 25°C) under natural light settings in the biology department of the University of Osnabrück. Two weeks before experimentation, animals (ca. 10 g fresh mass, FM) obtained from the large tank were divided into groups and transferred into three 2 l containers (placed within the big tank), which contained mussel grit and artificial seawater (ASW; Reef Salt, Aqua Medic GmbH, Bissendorf, Germany), adjusted to 32‰ salinity and pH 8.2. Animals were fed 3 times per week with tropical fish food (Ultra LPS, Fauna Marine GmbH, Holzgartingen, Germany), but starved 12 h before experimentation. Every second day the water was replaced.

Excretion experiments

For all excretion experiments, animals (ca. 0.3–0.4 g FM, 0.5–2 cm length) were transferred into small glass containers filled with 4 ml freshly prepared ASW and ca. 3 g of sterilized mussel grit as a hiding substrate. Experiments were performed in a darkened water bath (25°C). After an initial equilibration period (30 min), the container was rinsed 2 times (washing step) with ASW and refilled with 4 ml of fresh ASW for the first sampling period (control). An experimental sampling period and a final, second control sampling period followed. Between each sampling period (1 h), a washing step was conducted. At the end of each sampling period, two samples of 1.9 ml were taken from the containers for later analysis. For evaluation of the procedures, prior to each experimental treatment five individual animals were exposed to the experimental conditions (e.g. pH or pharmacological agents) to ensure full recovery after a 1 h exposure period. As acetazolamide, 5-(*N*-ethyl-*N*-isopropyl)amiloride (EIPA), KH7 and KM91104 needed to be dissolved in DMSO (final concentration, 0.1%), DMSO was also added to ASW for the respective control steps. All solutions employing inhibitors were adjusted to pH 8.2 by HCl or NaOH. For pH exposure experiments, ASW was adjusted to pH 6 and 9 with 5 mmol l^{-1} Trizma base and Hepes, respectively.

High environmental ammonia (HEA)

In a set of experiments to assess the polychaete's compensatory response to chronic (1 week) and acute (1 h) high ammonia exposure, *E. complanata* were placed into six separate 2 l containers, filled with mussel grit and either ASW or ASW enriched with 1 mmol l^{-1} NH_4Cl (HEA, 25°C, pH 8.2). Animals were fed every second day while ASW was replaced daily to keep the conditions as constant as possible. Animals were also starved 12 h prior to experimentation. For all experiments, animals were taken randomly from the respective tanks.

Ammonia determination

The ammonia content of ASW samples was measured using a gas-sensitive NH_3 electrode (Orion 9512, Thermo Scientific, Cambridge, UK) connected to a digital mV/pH meter, following the procedure established by Weihrauch et al. (1998). All samples were diluted 1:4 with ion-free water. Solutions for the standard curve were made according to the specific composition of the respective samples (e.g. pH or pharmacological agent), containing a range between 10 and 50 µmol l^{-1} NH_4Cl. Measurements were highly accurate with $R^2 \geq 0.99$.

Immunohistochemistry and western blot

Animals were anesthetized using an isotonic solution of $MgCl_2$ (approximately 8% $MgCl_2 \cdot 6H_2O$ w/v) in distilled water, and once immobile were fixed in 4% paraformaldehyde in phosphate-buffered saline (PBS: 140 mmol l^{-1} NaCl, 6.5 mmol l^{-1} KCl, 2.5 mmol l^{-1} Na_2HPO_4, 1.5 mmol l^{-1} KH_2PO_4, 12% sucrose, pH 7.4, 4°C, 2.5 h). After fixation specimens were rinsed in PBST (PBS+0.1% Tween) for 2 h or overnight. Prior to immunolabeling, specimens were dissected and single parapodia or segments were further processed. To increase permeability, they were treated with collagenase for 1.5 h (1000 U ml^{-1} collagenase Type VII, Sigma; in 1 mmol l^{-1} $CaCl_2$, 0.1% Triton X-100, 0.1 mol l^{-1} Tris/HCl buffer pH 7.5) followed by PBST+1% Tween and 1% Triton X-100 for 2 h. Specimens were rinsed with PBST then incubated with PBST containing 0.1% bovine serum albumin for 1 h, rinsed in PBST and incubated with primary antibodies for 2–4 days at 4°C. Primary antibodies were mouse anti-acetylated α-tubulin (monoclonal, Sigma-Aldrich, Heidelberg, Germany; dilution 1:1.000) and guinea pig anti-V-ATPase (polyclonal, subunit B specific; dilution 1:100; Weng et al., 2003). Following washing (3× in PBST, 20 min each), secondary antibodies were applied for 2–3 days at 4°C (depending on the respective primary antibodies: goat anti-mouse, Cy2 conjugated; goat anti-rabbit, Cy2 conjugated; goat anti-rabbit, Cy3 conjugated; or goat anti-guinea pig, Cy3 conjugated; Dianova, Hamburg, Germany; dilution 1:100). After being rinsed several times and washed in PBST overnight, specimens were mounted in Fluoromount (Southern Biotech, Birmingham, AL, USA). For visualizing the musculature, specimens were incubated in fluorescein isothiocyanate-labeled phalloidin for 1 h (100 µg per 5 ml ethanol; diluted 1:50 in PBS) and washed and embedded as described above. Confocal images

Journal of Experimental Biology

were captured with a LSM 5 Pascal confocal microscope (Zeiss, Jena, Germany). *Z*-stacks are displayed as maximum projections if not stated otherwise. Specificity of immunoreactivity was controlled by incubating specimens in the same manner, but omitting the primary antibodies.

Western blots were done essentially as described previously (Panz et al., 2012). Subsequent to homogenization (glass–Teflon homogenizer) and boiling (3 min, 99°C), total protein extracts (10 µg per lane) were separated by SDS-PAGE (17%) and transferred to nitrocellulose membranes (Carl Roth, Karlsruhe, Germany). Primary antibodies (anti-V-ATPase, polyclonal from guinea pig, subunit B specific; Weng et al., 2003) were applied at a dilution of 1:500, and secondary antibodies [goat anti-guinea pig IgG (whole molecule)-alkaline phosphatase conjugate, Sigma-Aldrich] at a dilution of 1:10,000.

Electron microscopy

For electron microscopy, specimens were fixed in a phosphate-buffered mixture of sucrose, picric acid, glutaraldehyde and paraformaldehyde (SPAFG) (Ermak and Eakin, 1976) for 2.5 h at 4°C and rinsed in phosphate buffer adjusted to the osmolarity of seawater (4°C, pH 7.2, 12% sucrose). Post-fixation occurred in 1% OsO_4 for 1 h (phosphate buffered as above) and dehydrated in a graded ethanol series. For SEM, specimens were then critical point dried with CO_2 and mounted on aluminium stubs, sputter coated with gold-palladium and examined with a Zeiss Auriga scanning electron microscope. For transmission electronmicroscopy (TEM), after dehydration, specimens were stepwise transferred into the intermedium propylene oxide (ethanol and propylene oxide 1:1, pure propylene oxide). Infiltration was in a mixture of the embedding medium and propylene oxide (1:3) overnight. Specimens were embedded in a mixture of Araldite and PolyBed 812. Polymerization was carried out at 60°C for 72 h. Ultrathin sections of the branchiae (70 nm) were made using a diamond knife on a Leica Ultracut E or Leica EM UC 6. Sections were mounted on single slot grids, contrasted with 2% uranyl acetate and 0.5% lead citrate for 30 and 20 min, respectively, in a Nanofilm Surface Analysis ultrastainer. Sections were examined with a Zeiss EM 902A transmission electron microscope operated at 50 or 80 kV. Micrographs were taken using a 4 K CCD camera (TRS, Moorenweis, Germany). Images were further processed using Image SP, Adobe Photoshop© and Illustrator©.

Quantitative PCR (qPCR)

Total RNA extractions were accomplished using Trizol (Invitrogen, Carlsbad, CA, USA) in an RNase-free environment, followed by DNase digestion using DNAse I (Invitrogen). Branchiae from control and HEA-exposed animals (see above) were isolated, as well as bodies stripped of their branchiae. The quality of total RNA was checked by gel electrophoresis and by Nano-drop measurement from the 260 nm:280 nm and 230 nm:280 nm ratio. Before transcription, RNA was treated with DNase I, followed by PCR (40 cycles) targeting GAPDH (see Table 1) to verify the absence of genomic DNA. Complementary DNA was synthesized using MonsterScript™ (Epicentre, Madison, WI, USA). Quantitative PCR was performed in a 2-step protocol with the annealing temperature set to 57°C. Prior to qPCR, a regular PCR was performed employing qPCR primers for all target genes. The resulting single PCR products were sequenced to confirm specificity. For the standard curve, defined amounts of amplified PCR products were used. GAPDH served as the reference gene as mRNA expression levels were similar between tissues and did not change upon treatments (data not shown). Primer sequences, PCR product sizes and the references gene-sequences accession numbers are provided in Table 1.

Phylogenetic analysis of Rh-glycoproteins and ammonia transporters (AMTs)

The Rh-protein and AMT data set contained 39 protein sequences. Amino acid sequences were aligned by MUSCLE alignment in MEGA 6. The most appropriate phylogenetic analysis model from 56 available models was determined utilizing the Mega 6 best model function. Phylogenetic analysis of MUSCLE aligned sequences was then performed in MEGA 6 using the maximum likelihood method with the LG+four categories of gamma substitution rates+invariable sites model and Nearest Neighbor Interchange (NNI) Heuristic Method. Bootstrap values were determined from 1000 bootstrap replicates.

Statistics

In this study, each *N* value represents the combined pool of polychaetes of ca. 0.3–0.4 g FM for transport experiments and ca. 0.3 mg of total pooled tissues for RNA isolation. Values from all experiments are specified as the mean±s.e.m. Significance ($P \leq 0.05$) between controls and treatments is indicated by asterisks. Statistical methods for the individual experiments are provided in the figure legends.

RESULTS

The ammonia excretion rate in *E. complanata* under control conditions (pH 8.2) accounted for 0.38±0.026 µmol g^{-1} FM h^{-1} (N=39). The excretion was constant over a time period of at least 3 h; however, when mussel grit was omitted from the test containers, excretion rates increased by ca. 55.3% (N=4, data not shown). This was most likely stress related, as prolonged rearing on plain glass (no hiding possibilities) led to a loss of their bristles. In order to evaluate whether the excretion rates depended on the environmental pH, whole animals were placed into ASW buffered to pH 8.2

Table 1. Primers employed in qPCR

Gene	Sense primer 5′→3′	Antisense primer 5′→3′	Product size (bp)	GenBank no.
GAPDH	CATCATTCCTGCATCCACTG	ATACTGCTATGCGTGTCCCC	267	KX421092
NKA	GACAACACTGTGATGGGACG	AGAACGACACACCCAGGAAC	133	KX421091
HAT	TCCCTGACTTGACGGGTTAC	GGATACATCAGCGTGGTCCT	164	KX421094
CA-2	ACGGACCTGATGTCCAAGAC	TCCAACTGTGCCTCTGACAC	197	KX421093
EcRhp1b	GTGTTTGGGGCATACTTTGG	ACACCCAGAGGAAGACGGTA	133	KX421088
EcAMT1	TCAGCTGTCTCAAATGCAGAA	GTTGGTGGTGTTTTTGCTCC	151	KX458239
EcAMT3	GCGGCGGTATCTACTGTCAT	ATGTGACAGACACAAGGGCA	136	KX421089
EcAMT4	TGGATATCGCAATTGGTTCA	CTTGATATGCCAAGCCCAAT	205	KX421090

Primers targeted GAPDH, Na^+/K^+-ATPase (NKA; α-subunit), V-type H^+-ATPase (HAT; subunit B), carbonic anhydrase isoform 2 (CA-2), Rhesus-like (Rh) ammonia transporter (EcRhp1b), and ammonia transporters EcAMT1, EcAMT3 and EcAMT4 from the marine polychaete *Eurythoe complanata*.

Journal of Experimental Biology (2017) 220, 425-436 doi:10.1242/jeb.145615

(control), pH 6 or pH 9 for 1 h. When exposed to ASW adjusted to pH 6, the excretion rate was not different from that of controls (Fig. 1A). In contrast, when exposed to pH 9, excretion rates decreased by approximately 40%. When the animals were placed back into control media (pH 8.2) after 1 h of exposure, increased levels of excretion were observed, suggesting a release of accumulated ammonia from the blood (Fig. 1B).

Mode of ammonia excretion

Because it was assumed that at least part of the animals' ammonia excretion occurs over epithelia directly facing the environment, in the next series of experiments, animals were exposed to a variety of different pharmacological agents to gather information regarding the nature of the excretion mechanism. Application of 5 µmol l^{-1} of the HAT inhibitor KM91104 and 2 mmol l^{-1} acetazolamide, an inhibitor of carbonic anhydrase (CA), caused a significant increase of the excretion rates by approximately 1.2- and 1.5-fold, respectively (Fig. 2A). Exposure to 100 µmol l^{-1} EIPA, a blocker of NHEs, and 0.5 mmol l^{-1} colchicine, a destabilizer of the microtubule network, had no effect on ammonia excretion rates in the polychaete (Fig. 2A). In the next series of experiments, we tested whether ammonia excretion is influenced by cAMP, a secondary messenger. Ammonia excretion was significantly activated by 10 µmol l^{-1} KH7, a selective inhibitor of soluble adenylyl cyclase, but partly inhibited by elevated intracellular cAMP levels induced by application of either 25 µmol l^{-1} 8-bromo-cAMP or 1 mmol l^{-1} of the phosphodiesterase inhibitor theophylline (Fig. 2B). After the wash-out step in the third sampling period, the effects of KM91104, acetazolamide, 8-bromo-cAMP and KH7 continued, while omitting theophylline caused a partial return to the initial control excretion rates (data not shown).

Characterization of the branchiae (gills)

In *E. complanata*, a pair of branchiae are present on each segment from the anterior end throughout the entire body. The branchiae are situated at the notopodia close to the dorsal cirrus and immediately behind the bundle of notochaetae (Fig. 3B).

The branchiae are dentrically branched and comprise a dorsal and a ventral tuft of flattened branches (Fig. 3C). These branches are about 100–200 µm long, 30–50 µm wide and up to 25 µm thick. Each branch is supplied with a band of densely arranged motile cilia at its narrow edges (Fig. 3D). In living animals, the cilia are continuously beating when observed under a light microscope. In addition, there are several tufts of short cilia present on the flattened surface of the branchiae (Fig. 3D). These cilia are immotile and belong to primary receptor cells; innervation and receptor cells are described in Purschke et al. (2016). The branchiae are primarily epidermal structures comprising only a few cell types, including unciliated supportive cells and ciliated cells forming the ciliary bands mentioned above (Fig. 3E). The epidermis is covered by a collagenous cuticle, which is thinner than the cuticle on the trunk (Fig. 3E; Purschke et al., 2016). The branchiae are supplied with a well-developed musculature comprising longitudinal and circular fibers (Fig. 3F), which largely follow the course of the main vessels. The branchiae are well vascularized and the main vessels give rise to numerous branches, which extend close to the surface (Fig. 3E,G). So, the blood is covered by epidermal cells less than 1 µm thick. Because of the presence of blood vessels, the branchiae appear reddish in color in living animals or fresh fixed material. Endothelial cells are lacking and the blood spaces are only lined by the extracellular matrix (ECM) separating adjacent epithelial cells (Fig. 3G). The branchiae are covered by a comparatively thin collagenous cuticle (1.8±0.3 µm), which is traversed by numerous epidermal microvilli. The microvilli have a diameter of ca. 35 nm with 18±4 microvilli µm^{-2} surface (Fig. 3E,G).

To further verify that the described branchiae are a potential site for ammonia excretion, it was assessed whether transcripts of proteins commonly found to be responsible for gas exchange and ammonia excretion are expressed. For this, the branchiae were isolated and mRNA expression levels of key transporters/enzymes were compared with expression levels in the main body that had been stripped of the branchiae. The results showed that carbonic anhydrase isoform 2 (CA-2, cytoplasmic isoform), NKA (α-subunit) and HAT (subunit B) were, respectively, approximately 11, 4 and 4 times higher expressed in the branchiae compared with the remaining body (Fig. 4A). One Rh-protein was identified in the branchiae and named EcRhp1b (GenBank accession no. KX421088). Note, Ec stands for the species name, while Rhp1 stands for the invertebrate primitive Rh-protein cluster. EcRhp1b revealed a 4-fold higher mRNA abundance in the branchiae compared with the body (Fig. 4B). All absolute mRNA expression values of control polychaetes can be found in Table 2. In addition to the Rh-protein, three transcripts were identified coding for proteins clustering with AMTs from plants, methylamine permeases (Meps) from fungi and AMTs from other invertebrates (Fig. 5). These putative ammonia transporters were named EcAMT1 (GenBank accession no. KX458239), EcAMT3 (GenBank accession no. KX421089) and EcAMT4 (GenBank accession no. KX421090), according to their sequence similarities to AMTs expressed in *Caenorhabditis elegans*. All AMTs exhibited higher abundance in the branchiae when compared with the main body, with approximately 58, 6 and 12 times higher relative mRNA expression for EcAMT1, EcAMT3 and EcAMT4, respectively (Fig. 4B). Note, as shown in Table 2, qPCR revealed that transcript levels of EcAMT4 are extraordinarily high in the branchiae, with approximately 8 and 4 times greater absolute abundance compared with transcript levels detected for NKA (α-subunit) and EcRhp1b, respectively.

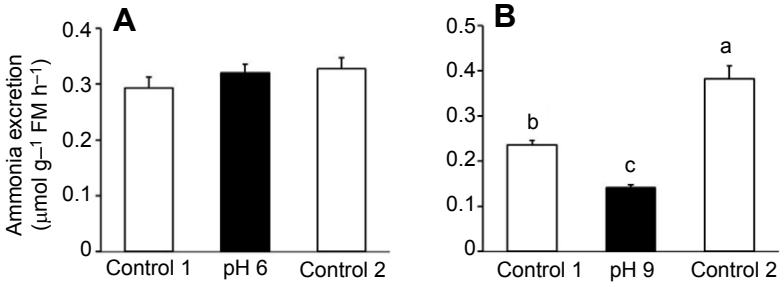

Fig. 1. Ammonia excretion rates in *Eurythoe complanata* exposed to different pH regimes. Ammonia excretion rates were sampled over three consecutive hours. In the second sampling period, the artificial seawater (ASW) was adjusted to either pH 6 (A) or pH 9 (B). Significant differences are indicated by different letters. Data were analyzed by one-way ANOVA with repeated measures using a Tukey's pairwise comparison (means±s.e.m., *N*=4).

Journal of Experimental Biology (2017) 220, 425-436 doi:10.1242/jeb.145615

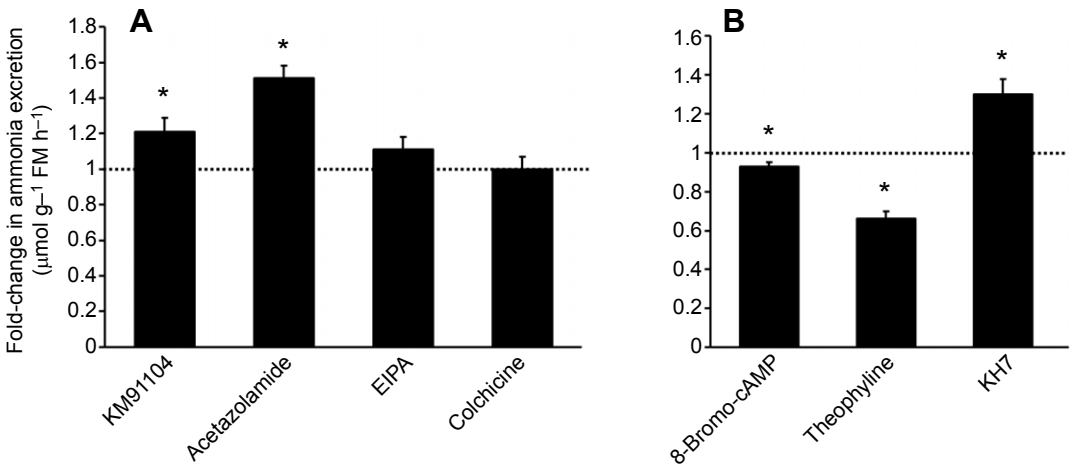

Fig. 2. Effects of different inhibitors and modulators of cellular cAMP levels on ammonia excretion rates in *E. complanata*. (A) Inhibitor concentrations and target (in parentheses) were: KM91104 (V-ATPase), 5 μmol l^{-1} (*N*=4); acetazolamide (carbonic anhydrase), 2 mmol l^{-1} (*N*=4); EIPA (cation/H^+-exchanger), 100 μmol l^{-1} (*N*=4); and colchicine (microtubule network), 0.5 mmol l^{-1} (*N*=4). (B) cAMP modulator concentrations and target (in parentheses) were: 8-bromo-cAMP (intracellular cAMP levels), 25 μmol l^{-1} (*N*=4); theophylline (phosphodiesterase), 1 mmol l^{-1} (*N*=4); and KH7 (soluble adenylyl cyclase), 10 μmol l^{-1} (*N*=4). Control values for each treatment were set to 1 (dotted line), with values measured under the influence of the agents given as fold change of the respective control. Significant differences from the respective control values are indicated by asterisks. Data were analyzed by paired Student's *t*-test (two-tailed) on excretion rates prior to calculation of fold-change values (means±s.e.m.).

Localization of HAT

As HAT is a key player in ammonia transport processes, the presence and localization of the multi-subunit enzyme within the branchiae was analyzed by means of immunohistochemistry. We utilized polyclonal antibodies raised against subunit B of the tobacco hornworm *Manduca sexta* HAT (Weng et al., 2003). In order to confirm specificity of the antiserum in *E. complanata*, western blots were performed with total protein extracts isolated from adult animals. As shown in Fig. 6A, application of the respective antiserum resulted in detection of a single protein with a molecular mass of about 55 kDa, which corresponds well to the expected subunit B mass of 56 kDa (Weng et al., 2003). These data strongly indicate that the applied antiserum specifically detects subunit B of the *E. complanata* HAT. Utilizing the respective antiserum in tissue staining revealed that within the branchiae, HAT localizes to basolateral membranes of the single-cell layer epithelium. In addition to this localization, a second signal is apparent in a patchy manner within the cytoplasm, presumably representing vesicles containing HAT (Fig. 6B).

Effects of HEA

In the next series of experiments, animals were exposed for 1 week either to control ASW (pH 8.2) or to ASW enriched with 1 mmol l^{-1} NH_4Cl (HEA, pH 8.2) to assess potential changes in ammonia excretion rates and mRNA expression levels of key proteins involved in the transport mechanism.

When control animals were exposed acutely for 1 h to HEA, ammonia excretion reversed to become ammonia uptake. After re-exposure to ammonia-free ASW, ammonia excretion was re-established, but with a significantly higher rate compared with the initial control excretion value (Fig. 7A). When animals exposed to HEA for 1 week were placed in ammonia-free ASW, the excretion rates were 1.94±0.14 μmol g^{-1} FM h^{-1}, about 3 times as high as rates measured in control animals (0.75±0.06 μmol g^{-1} FM h^{-1}). Notably, when animals were subsequently exposed to HEA (acclimation media), excretion rates were 0.75±0.32 μmol g^{-1} FM h^{-1}, basically identical to the excretion rates measured in control animals in ammonia-free ASW (Fig. 7A,B). Chronic exposure to HEA also caused an increase in mRNA levels in the body (stripped of branchiae) for NKA (α-subunit) and CA-2, and showed a tendency for increased EcAMT1 mRNA, whereas mRNA expression levels of HAT (subunit B), EcRhp1b, EcAMT3 and EcAMT4 remained unchanged. HEA also caused a differential expression pattern of some target genes in the branchiae. Whereas relative mRNA expression levels of NKA and EcRhp1b did not change, HAT showed a tendency to be up-regulated. CA-2 and all AMTs tended to be down-regulated compared with expression levels found in the branchiae of control animals (Fig. 8).

DISCUSSION

The branchiae

Despite a general diversity in terms of position, external structure and occurrence of branchiae in annelids, certain common characters are apparent, which likewise can be observed in the amphinomid *E. complanata* (Gardiner, 1988; Rouse and Pleijel, 2001). Most polychaete branchiae studied so far are equipped with motile cilia, which are arranged in bands, clusters or tufts, effecting continuous and strong water currents (Gardiner, 1988). Likewise, the epidermis and cuticle are always thinner than in other parts of the body. It should be noted that the annelid cuticle is a soft and flexible, rather than tight, border and is typically traversed by numerous microvilli (Hausen, 2005; Purschke et al., 2014). Mostly, annelid branchiae are supplied with efferent and afferent vessels, which give rise to some kind of connecting vessel and often blind-ended blood spaces extending deeply into the epidermal cells. The distance between the blood spaces and the external medium has usually been reported to be as little as 1 μm but can exceed 7–10 μm (Gardiner, 1988). Other studies report a thickness of epidermal cells covering the blood spaces of the same order as observed in the present investigation, which is among the smallest diffusion distances reported so far, e.g. in *Diopatra neopolitana* (Menendez et al., 1984). As is typical for annelids and invertebrates, in general these vessels represent spaces in the ECM of adjacent epithelia (Fransen, 1988; Westheide, 1997). The absence of a well-developed basal labyrinth system, usually

Journal of Experimental Biology (2017) 220, 425-436 doi:10.1242/jeb.145615

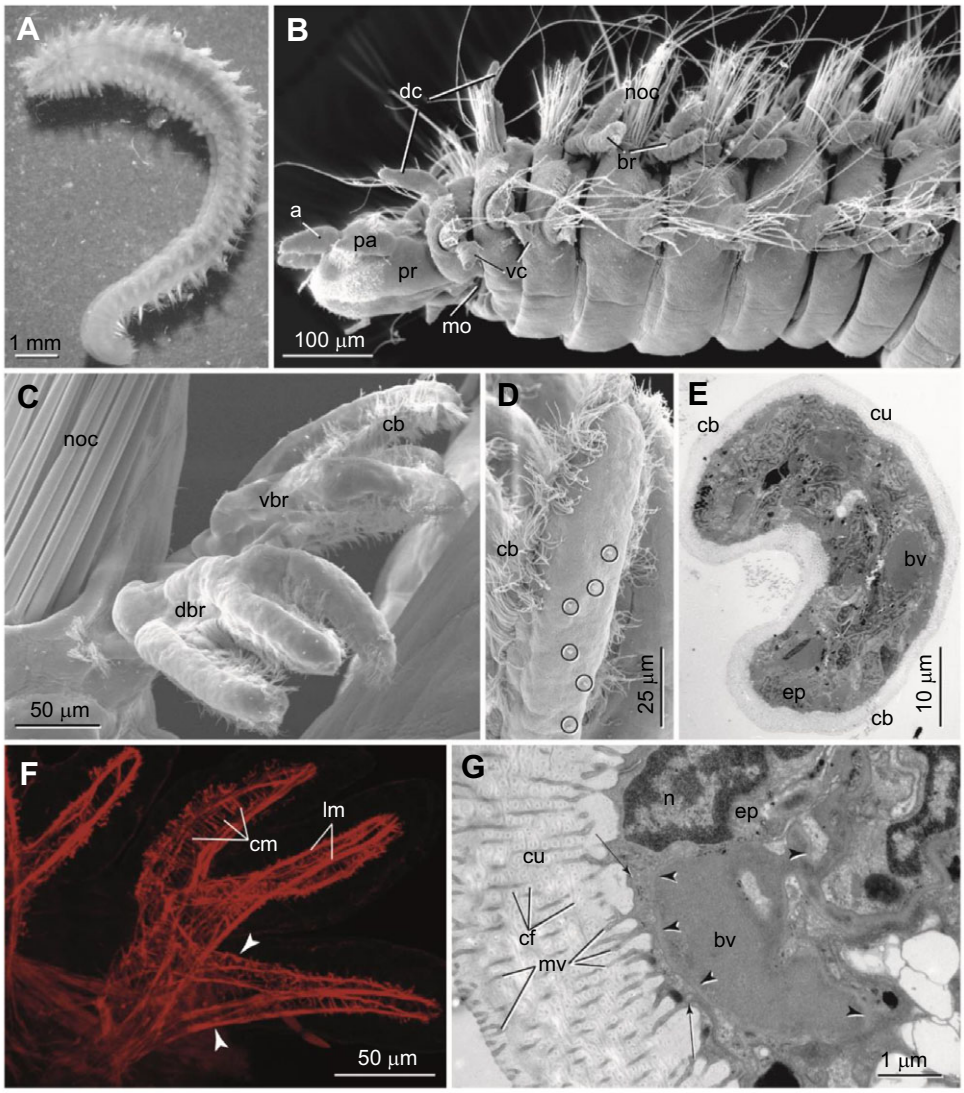

Fig. 3. Morphology and position of branchiae in *E. complanata*. (A) Entire living animal under light microscopy. (B) Anterior end in lateral view by scanning electron microscopy (SEM) showing parapodia with dorsal (dc) and ventral cirri (vc) and branchiae (br) well protected between notochaetae (noc); a, antenna; mo, mouth; pa, palp; pr, prostomium. (C) SEM enlargement of single branchia branching into dorsal (dbr) and ventral (vbr) group of branchial filaments; each filament has a ciliary band (cb) on the narrow side; noc, notochaetae. (D) SEM enlargement of a single branchial filament with a continuous ciliary band (cb) surrounding the entire filament; the receptor cell cilia are encircled. (E) Micrograph from low-power transmission electron microscopy (TEM) showing the entire branchial branch in cross-section with ciliary bands (cb), blood vessels (bv), epidermis (ep) and thin cuticle (cu). (F) Branchia stained with phalloidin against actin (red) by confocal laser-scanning microscopy; each branch is supplied with intrinsic musculature. Musculature of the branchiae is composed of strong longitudinal (lm) and fine circular fibers (cm) following the course of blood vessels, forming a hairpin (arrowheads). (G) TEM of blood space (bv) and connection to deeper regions through spaces in the extracellular matrix (ECM); arrowheads point to continuous ECM surrounding the blood; arrows point to thin epidermal cover measuring 130–350 nm. Cuticle (cu) on branchia is traversed and extended by branching microvilli (mv); collagen fibers (cf) form a loose network.

characteristic of actively transporting cells, led certain authors to conclude that branchiae do not have additional functions such as osmoregulation or excretion (Gardiner, 1988; Storch and Alberti, 1978). As a basal labyrinth system has not been observed either in *E. complanata* or other annelids, additional studies were needed to clarify whether they have additional functions. Gene expression studies conducted in the current investigation support the notion that ammonia excretion and acid–base regulation are at least partly accomplished by the branchiae in *E. complanata*. High branchial mRNA expression levels of NKA, HAT, CA-2 and a Rh-protein, all genes known to be involved in ammonia excretion and acid–base regulation (Larsen et al., 2014), as well as the observed ultrastructure of the tissue, which features traits of typical branchiae/gills of osmoconforming invertebrates (Gardiner, 1992; Smith, 1992), provide indirect but strong evidence for this assumption.

Of particular interest was the identification and branchial expression of three AMTs, proteins best known as the main transporters for NH_4^+ uptake in plant roots (Ludewig et al., 2002). Although AMTs have not so far been shown to be expressed in vertebrates, transcriptome projects have revealed that AMTs are expressed in invertebrates, clustering closer to the high-affinity transporters (AMT1 family) found in plants than to the fungal MEPs and bacterial AmtBs (Fig. 5). To our knowledge, only two studies, both on mosquitoes, have investigated the function and role of AMTs in invertebrate species. While a functional study on adult *Anopheles gambiae* strongly suggested that AMTs in invertebrates mediate the transport of NH_4^+ (Pitts et al., 2014), a physiological study on the anal papillae of yellow fever mosquito *Aedes aegypti* larvae showed the importance of AMTs in the ammonia excretion process. Immunohistochemistry further revealed a basal localization of the AMT in the epithelium of the anal papillae (Chasiotis et al., 2016). As mentioned above, in *E. complanata*, transcripts of three different AMTs have been identified within the branchiae, exhibiting vastly different mRNA expression levels. Information regarding their cellular localization requires further studies; however, one can expect the presence of an AMT on either side of the gill epithelium because of its potential function as a pathway for NH_4^+. Moreover, with caution one could speculate that EcAMT4 is localized to the basolateral membrane, as its relatively high expression level compared with that of the Rh-protein is similar to findings in the anal papillae of *A. aegypti* (Chasiotis et al., 2016). The overall importance of EcAMT4 is further underlined by its absolute mRNA expression level in the branchiae, which was considerably higher than transcript levels found for the gill energizing pump, NKA, and for the major acid–base regulatory protein, CA-2.

Journal of Experimental Biology (2017) 220, 425-436 doi:10.1242/jeb.145615

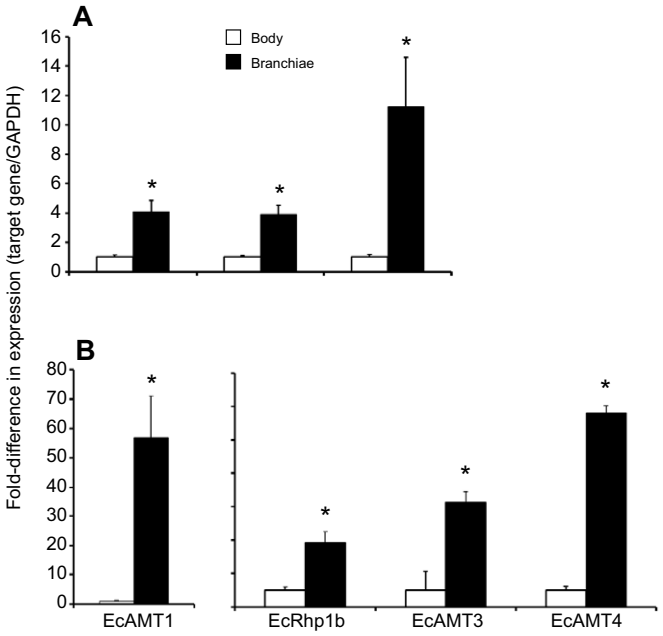

Fig. 4. Fold-difference in relative mRNA expression levels detected in the body and the branchiae in *E. complanata*. (A) Na^+/K^+-ATPase α-subunit (NKA, *N*=4), V-type H^+-ATPase subunit B (HAT, *N*=4) and cytoplasmic carbonic anhydrase 2 (CA-2, *N*=4). (B) Rhesus-like (Rh)-protein EcRhP1b (*N*=4), and ammonia transporters EcAMT1 (*N*=4), EcAMT3 (*N*=4) and EcAMT4 (*N*=4). Values for the body stripped of branchiae (open bars) were set to 1. Asterisks indicate a significant difference between the relative expression levels in the body and the branchiae. Data were analyzed by paired Student's *t*-test (two-tailed) on expression prior to calculation of fold-change values (means±s.e.m.).

Working model for the branchial ammonia excretion mechanism

In order to provide a basis for future studies and discussions, we integrated the information gained regarding the branchial ammonia excretion mechanism in *E. complanata* into a working model (Fig. 9). For this model, it is assumed that NH_4^+ is transported from the blood into the branchial epithelial cells in an active manner by the $Na^+/K^+(NH_4^+)$-ATPase. While no direct evidence could be provided in this study because of the lethality of the NKA inhibitor ouabain to *E. complanata*, this mechanism has been shown in other marine polychaetes, namely *Nereis succinea* and *Nereis virens*, but also for the ammonia transporting epithelia of many other vertebrates and invertebrates (Evans et al., 1989; Larsen et al., 2014; Mangum, 1978; Quijada-Rodriguez et al., 2015; Weihrauch et al., 1998; Mangum, 1978). Further, movement of NH_4^+ into cells may also be driven by the negative intracellular potential via a basolateral localized AMT, possibly EcAMT4. However, it is also very possible that the basolateral AMT instead serves as a NH_4^+ backflow valve to limit a cytoplasmic overload, similar to epithelial basolateral K^+-channels (Riestenpatt et al., 1996). Respiratory CO_2 might enter the cells via a basolaterally localized Rh-protein, which has for physiological systems been strongly suggested to function as a dual-gas channel, mediating the transport of NH_3 and CO_2 (Endeward et al., 2008; Kustu and Inwood, 2006; Perry et al., 2010; Soupene et al., 2004). Because of its high mRNA expression levels in the body, it is assumed that EcRhp1b is the basolateral localized 'housekeeping' transporter, similar to CeRhr-1, identified in the nematode *C. elegans* (Adlimoghaddam et al., 2015, 2016). As described below, EcRhp1b might serve as a NH_3 backflow channel, important for acid–base homeostasis (Fig. 9A). However, it cannot be excluded that the Rh-protein also provides an exit for NH_4^+, as recent studies demonstrated that at least some mammalian Rh-glycoproteins are capable of mediating the transport of both forms of ammonia (Caner et al., 2015). Apical exit of NH_4^+ is likely driven by the outwardly directed electrochemical gradient for NH_4^+ and probably mediated by an apically localized AMT. Apical ammonia trapping (acid trapping) via Rh-proteins, as suggested for ammonia excreting epithelia in freshwater invertebrates and fish (Larsen et al., 2014; Quijada-Rodriguez et al., 2015; Wright and Wood, 2009), is likely not of major importance in the excretory mechanisms of *E. complanata*. This is evident from the lack of an apical V-ATPase and the observed unaltered ammonia excretion rate when animals were exposed to an environment that was buffered to pH 6, a condition that, considering a physiological intracellular pH between 7.3 and 7.8, established a considerable outwardly directed P_{NH_3}. Moreover, because of the lack of inhibition upon application of colchicine, a vesicular microtubule-dependent ammonia excretion mechanism, as suggested to be functioning in gills of the green crab, *Carcinus maenas* (Weihrauch et al., 2002), and the hypodermis of the nematode *C. elegans* (Adlimoghaddam et al., 2015), is not assumed to be in place in *E. complanata*. In addition, the basolateral localization of HAT as well as the pharmacological experiments employing modulators of cellular cAMP levels suggest that the branchiae of *E. complanata* also exhibit a regulatory function that is set up to transport NH_3, in a secondary active manner, out of the cytoplasm back into the blood. HAT, localized in the basolateral membrane, likely generates a cytoplasm to blood-directed P_{NH_3} gradient by a steady acidification of the blood within the vessels in branchial tissue that consequently drives NH_3 out of the cell via EcRhp1b or simple membrane diffusion (Goldmann and Rottenberg, 1973). Supported by the reduced excretion rates after exposure to theophylline and 8-bromo-cAMP, HAT here is likely to be activated by intracellular cAMP as, for example, demonstrated for the assembly and activity of plasma membrane HAT in blowfly salivary glands (Dames et al., 2006) (Fig. 9A). Alternatively, intracellular cAMP may not directly activate HAT but instead signal for translocation of additional HAT-containing cytoplasmic vesicles to fuse with the basolateral membrane to increase the abundance of this protein, as seen in the gills of Pacific spiny dogfish *Squalus*

Table 2. Absolute mRNA expression levels

	NKA	HAT	CA-2	EcRhp1b	EcAMT1	EcAMT3	EcAMT4
Branchiae							
Mean±s.e.m.	1.0±0.12	0.1±0.025	1.44±0.23	2.1±0.2	0.013±0.004	0.43±0.08	8.5±2.2
N	4	5	4	5	5	5	5
Body							
Mean±s.e.m.	0.37±0.14	0.025±0.0028	0.25±0.06	0.72±0.19	0.0004±0.00011	0.14±0.05	0.76±0.32
N	4	4	4	4	5	5	4

Expression (in fg cDNA per 50 ng total RNA) of Na^+/K^+-ATPase α-subunit (NKA), V-type H^+-ATPase subunit B (HAT), carbonic anhydrase isoform 2 (CA-2), Rh-protein EcRhp1b, and ammonia transporters EcAMT1, EcAMT3 and EcAMT4 in the marine polychaete *Eurythoe complanata*.

Journal of Experimental Biology (2017) 220, 425-436 doi:10.1242/jeb.145615

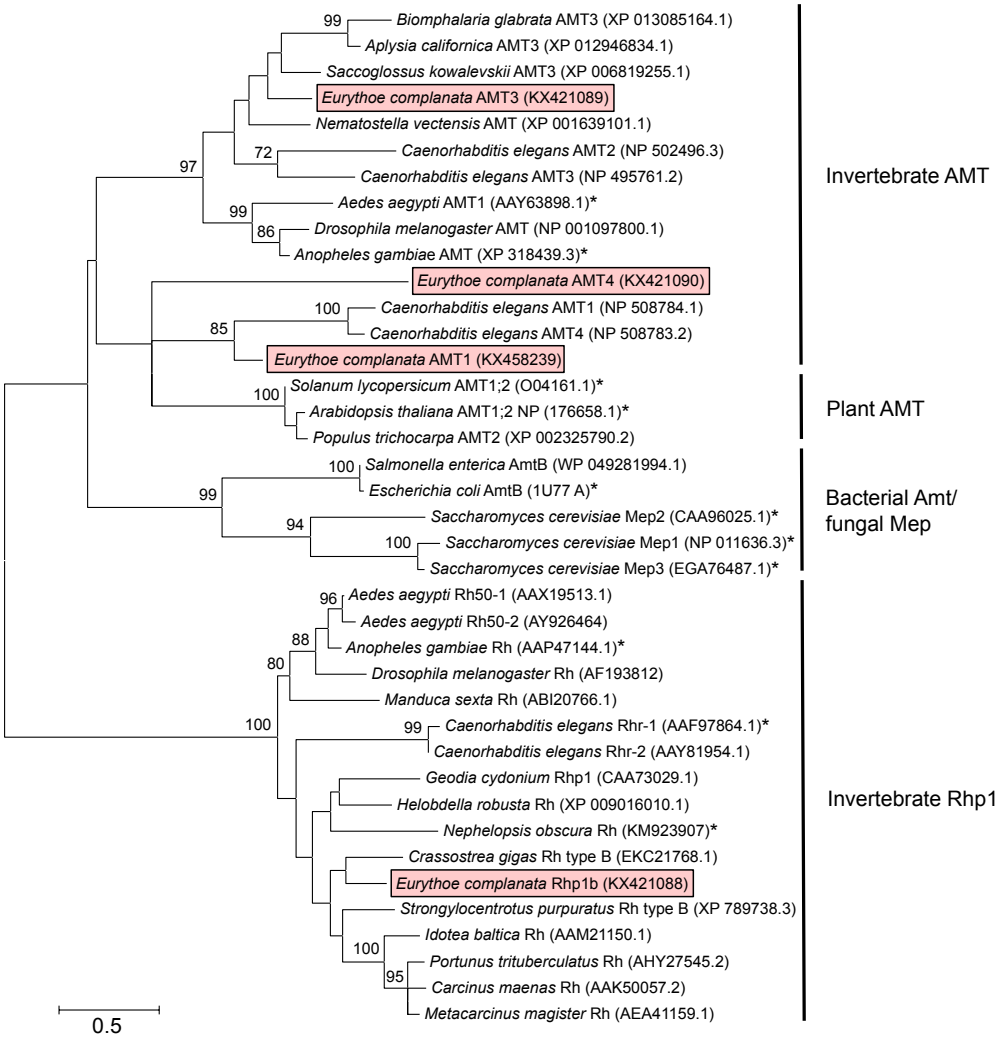

Fig. 5. Phylogenetic analysis of putative *E. complanata* Rh-protein and AMTs. Numbers beside branches represent bootstrap values from 1000 replicates. The tree branches are drawn to scale, with the scale bar representing the number of amino acid substitutions per site. Asterisks indicate sequences with a confirmed ammonia transport capability. GenBank accession numbers are given in parentheses following the species name and gene.

acanthias L. (Tresguerres et al., 2010). Consequently, a reduction of cellular cAMP levels by inhibiting the soluble adenylyl cyclase thereby reduces the amount of basolateral HAT and consequently causes a decrease of the acidification of the blood (Fig. 9B). A blood-directed ammonia transport was also observed in perfused gills of the marine cephalopod *Octopus vulgaris*, where hemolymph ammonia levels were maintained and adjusted by metabolically produced ammonia to approximately 300 µmol l^{-1} (M. Y. Hu, personal communication), when plasma levels were below that value. Further, a function of retaining ammonia in particular situations was also observed when *E. complanata* was exposed to a high environmental pH. Under this condition, it would be physiologically meaningful to reduce NH_4^+ excretion and retain the acid equivalent in order to maintain acid–base homeostasis. When animals were placed back

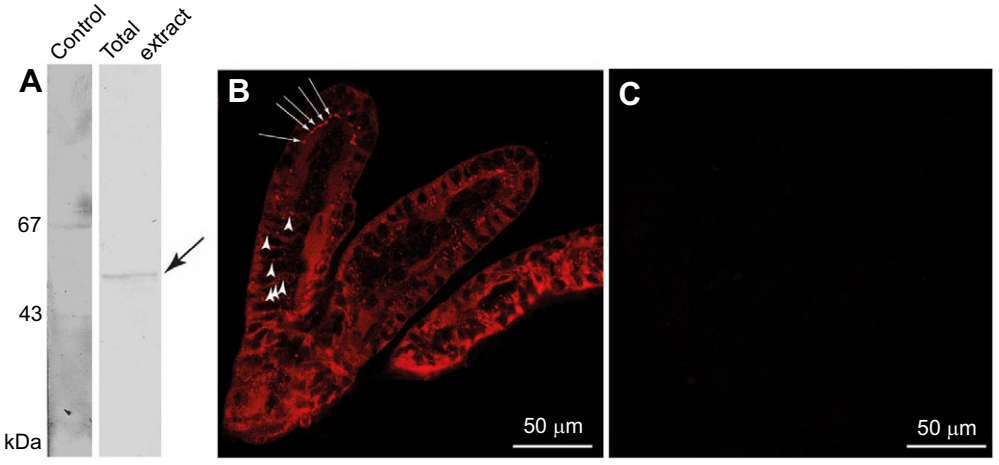

Fig. 6. Immunolocalization of the HAT in branchiae of adult *E. complanata*. (A) Western blot of total protein extract isolated from adult *E. complanata*. Application of anti-V-ATPase antibodies (subunit B specific) results in detection of a single protein of about 55 kDa (arrow) in the total protein extract. (B) Application of the same antibodies to parapodial appendice tissue results in detection of the HAT mainly in basolateral membranes (arrows). An additional signal is obvious in vesicular structures within the cytoplasm (arrowheads). (C) Control staining, lacking the primary antibody. No signal above background was observed.

Journal of Experimental Biology (2017) 220, 425-436 doi:10.1242/jeb.145615

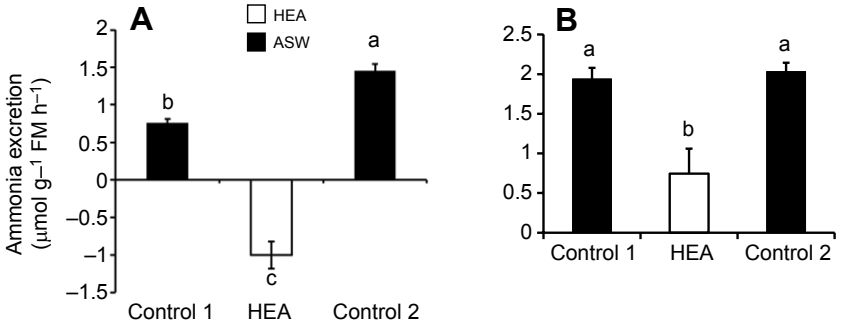

Fig. 7. Ammonia excretion rates. (A) *Eurythoe complanata* were acclimated to control ASW, followed by acute (1 h) exposure to HEA (1 mmol l^{-1} NH_4Cl) and a subsequent return to control conditions. (B) *Eurythoe complanata* that had been chronically exposed to HEA (1 week, 1 mmol l^{-1} NH_4Cl) were placed in ammonia-free ASW, followed by re-exposure to HEA and a subsequent return to control conditions. Significant differences are indicated by different letters. Data were analyzed by one-way ANOVA with repeated measures using a Tukey's pairwise comparison (means±s.e.m., *N*=4).

into control ASW (pH 8.2), excess ammonia was excreted at an increased rate to rid accumulated blood ammonia. Finally, the high influx rate upon a short-term exposure to elevated environmental NH_4Cl concentrations indicates further that the paracellular pathway for ammonia also plays a role in transepithelial ammonia fluxes.

As an alternative to the backflow hypothesis, it is plausible that the protons pumped into the blood by HAT work to trap ammonia in the blood as NH_4^+. This action would thereby reduce NH_3 excretion into the cytoplasm of the cells rather than drive a backflow of NH_3 from cell to blood as proposed above. Here, a reduction in NH_3 flux would essentially still aid in an ammonia retention as was also proposed in the ammonia backflow hypothesis above. In order to distinguish between these two hypothetical mechanisms, further studies will be required to localize transporters and determine intracellular and extracellular pH/ammonia concentrations to assess the feasibility of ammonia backflow.

Exposure to HEA

As a burrowing animal, it is likely that *E. complanata* experiences elevated environmental ammonia levels from time to time as a result of an accumulation of metabolically released ammonia while in the burrow (Weihrauch et al., 1999). Acute exposure to 1 mmol l^{-1} ammonia caused a rapid uptake of ammonia. This is to be expected as the coelomic fluid of another marine polychaete, the lugworm, *Arenicola marina*, contains approximately 550 μmol l^{-1} ammonia (Reitze and Schöttler, 1989); therefore, during a 1 mmol l^{-1} ammonia exposure, an inwardly directed ammonia gradient would likely be present. Also, other marine invertebrates usually have fairly low hemolymph/blood ammonia concentrations ranging between approximately 100 and 300 μmol l^{-1}, as observed in crustaceans (Weihrauch et al., 2004), cephalopods (M. Y. Hu personal communication) and horseshoe crabs (S. Hans, personal communication), for example. The influx might also be facilitated by a high epithelial conductance as directly shown for the gill epithelium in *Cancer pagurus* (Weihrauch et al., 1999). However, after a 7 day acclimation to HEA, *E. complanata* was capable of excreting ammonia at control rates. When exposed to regular ASW, excretion rates tripled, indicating that blood ammonia concentrations in HEA-acclimated polychaetes were above environmental levels. Given that blood ammonia was not assessed, this assumption is speculative but is nevertheless supported by the fact that transcript levels of several genes (NKA and CA-2, and a tendency for EcAMT1 and EcAMT3) potentially involved in ammonia transport processes are up-regulated within the body. As presumably internal organs are exposed to elevated blood ammonia levels, a higher abundance of these genes might protect the body cells from toxic effects. Alternatively, the observed increase in mRNA expression in the body could be indicative of another ammonia transporting epithelium playing a greater role during HEA exposure, such as the metanephiridia and/or intestine, both previously shown in annelids to transport ammonia (Kulkarni et al., 1989; Tillinghast, 1967; Tillinghast et al., 2001). In contrast to the branchiae, neither the

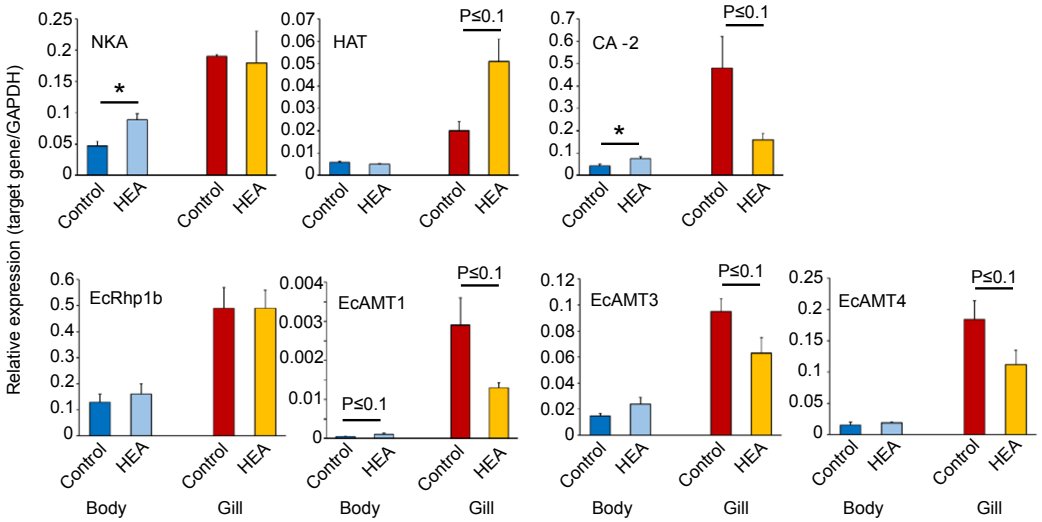

Fig. 8. Relative mRNA expression of target proteins in the body and branchiae in control (ASW) and HEA (1 mmol l^{-1} NH_4Cl)-acclimated *E. complanata*. Body values are represented by dark and light blue bars, branchiae by red and orange bars. NKA, *N*=4–5; HAT, *N*=4; CA-2, *N*=4–5; EcRhp1b, *N*=4–5; EcAMT1, *N*=4; EcAMT3, *N*=5; EcAMT4, *N*=4–5. Significant differences between control and HEA-acclimated animals are indicated by an asterisk. *P*≤0.1 indicates a *P*-value between 0.05 and 0.1 (trending; tendency). Data were analyzed by unpaired Student's *t*-test (two-tailed) (means±s.e.m.).

Journal of Experimental Biology (2017) 220, 425-436 doi:10.1242/jeb.145615

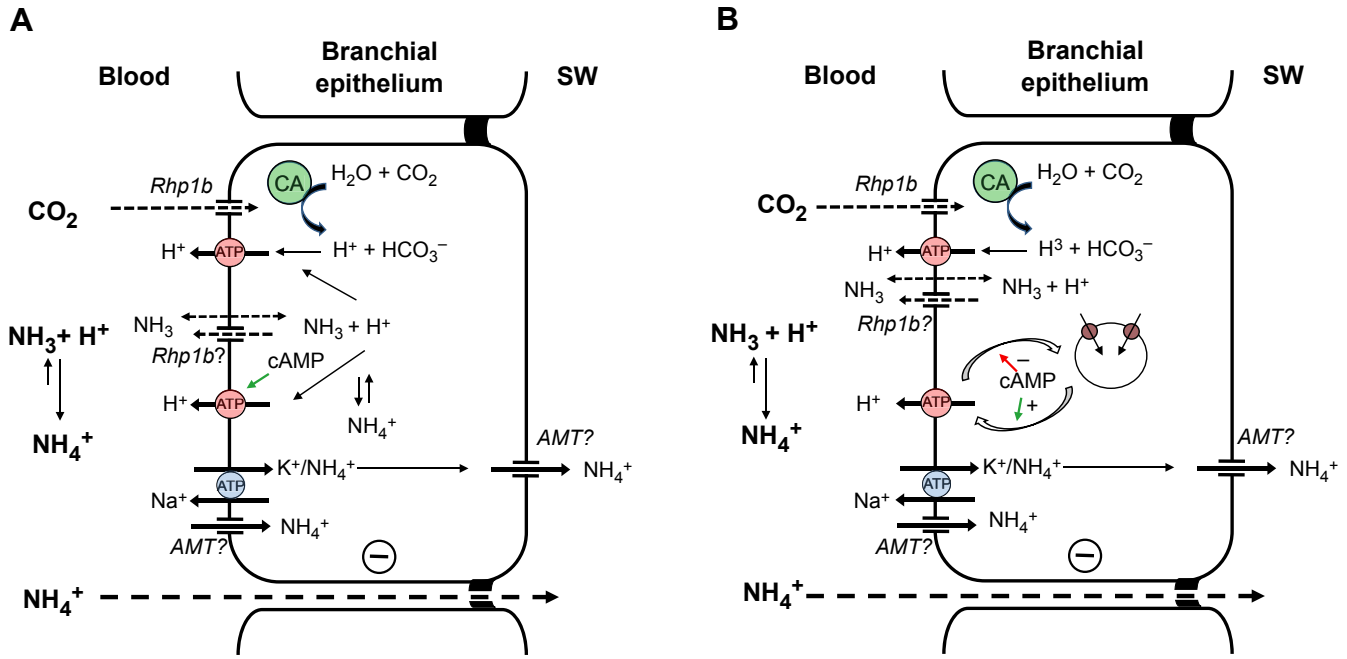

Fig. 9. Hypothetical working models of the ammonia transport pathways in the branchiae of *E. complanata*. For a description of the pathways, see Discussion. CA, cytoplasmic carbonic anhydrase. ? indicates speculative localization of transporter; the green arrow indicates indirect activation of HAT via cAMP or insertion of HAT carrying vesicles. Dashed arrows indicate a diffusive pathway of a gas or paracellular diffusion.

intestine nor the metanephridia is in direct contact with the environment and therefore they may be more readily capable of excreting ammonia unchallenged by the strong environmental ammonia gradient. Elevated transcript levels of a Rh-protein were also observed in various tissues of HEA (1 mmol l^{-1}, 2 weeks)-acclimated Dungeness crabs, *Metacarcinus magister*; in this case, hemolymph levels rose to nearly environmental concentrations (Martin et al., 2011). It is noteworthy that in HEA (1 mmol l^{-1} NH_4HCO_3)-exposed marine pufferfish, after an initial ammonia uptake, excretion returned after 12 h to control rates, while plasma ammonia concentrations increased from approximately 300 µmol l^{-1} to near environmental levels (Nawata et al., 2010).

Changes in transcript expression levels in the present study do not support the assumption that the observed ammonia excretion in HEA-enriched ASW was due to an activated/enhanced branchial excretion mechanism. In fact, with the exception of HAT, which showed a tendency to be up-regulated, the potential ammonia transporters EcAMT1, EcAMT3 and EcAMT4 had a tendency to be down-regulated. Regardless, if, as speculated above, the basolateral AMT also serves as a NH_4^+ backflow valve, to reduce the overload of intracellular ammonia, a down-regulation of this transporter would keep intracellular ammonia levels higher, thereby promoting excretion. However, as mentioned earlier, it could be that another ammonia transporting tissue (e.g. metanephridia and/or intestine) is activated and the branchiae may reduce ammonia transport capabilities to prevent ammonia influx through branchial tissues. More mechanistic studies as well as functional expression analysis for the Rh-proteins and all AMTs are required to make further statements regarding the ammonia excretion mechanism in HEA-acclimated *E. complanata*.

Conclusions

The study of invertebrates with regard to their nitrogen excretion mechanisms and tolerance of environmental stressors has been neglected in the past, despite their overall dominance (number of phyla and species) and ecological importance in the animal kingdom. By investigating marine invertebrates such as decapod crabs, cephalopods and, as in this case, marine polychaetes, it has become obvious that ammonia has an important role as an acid–base equivalent in aquatic animals (Fehsenfeld and Weihrauch, 2013, 2016; Hu et al., 2013). Ammonia, which can be actively excreted or retained within the body fluids, might very likely be crucial for blood pH homeostasis, particularly in animals exhibiting a very high ion conductance of their surface epithelia, such as marine invertebrates, where ammonia can easily leak out via the paracellular pathway into the environment.

Acknowledgements

We would like to thank Dr Helmut Wieczorek for providing the anti-V-ATPase subunit B antiserum.

Competing interests

The authors declare no competing or financial interests.

Author contributions

D.T. performed qPCR experiments and provided together with M.H. the first draft of the MS; M.H. performed TEM imaging as well as light microscopy; H.M. performed western blotting and IHC experiments; A.R.Q.-R. conducted phylogentic analysis of the obtained sequences and produced gene tree; G.P. performed SEM experiments and supervised TEM imaging; A.P. provided funding; D.W. performed transport experiments and supervised the project; all authors revised and approved the draft.

Funding

This work was supported by the Incentive Award of the Faculty of Biology/Chemistry (University of Osnabrück) to H.M., and by grants from the Deutsche Forschungsgemeinschaft to A.P. and H.M. (SFB 944). A.P. received additional funding from the State of Lower-Saxony, Hannover, Germany [11-76,251-99-15/12 (ZN2832)]. A.R.Q.-R. and D.W. were funded by the Natural Sciences and Engineering Research Council of Canada.

Data availability

Sequence information has been deposited in GenBank for: EcRhp1b (KX421088), EcAMT1 (KX458239), EcAMT3 (KX421089), EcAMT4 (KX421090), *Eurythoe*

complanata carbonic anhydrase type 2 (KX421093), *Eurythoe complanata* V-type proton ATPase subunit B (KX421094), *Eurythoe complanata* glyceraldehyde 3-phosphate dehydrogenase (KX421092) and *Eurythoe complanata* Na/K-ATPase alpha-subunit (KX421091).

References

Adlimoghaddam, A., Boeckstaens, M., Marini, A.-M., Treberg, J. R., Brassinga, A.-K. C. and Weihrauch, D. (2015). Ammonia excretion in *Caenorhabditis elegans*: mechanism and evidence of ammonia transport of the Rh-protein CeRhr-1. *J. Exp. Biol.* **218**, 675-683.

Adlimoghaddam, A., O'Donnell, M. J., Kormish, J., Banh, S., Treberg, J. R., Merz, D. and Weihrauch, D. (2016). Ammonia excretion in Caenorhabditis elegans: physiological and molecular characterization of the rhr-2 knock-out mutant. *Comp. Biochem. Physiol. A Mol. Integr. Physiol.* **195**, 46-54.

Caner, T., Abdulnour-Nakhoul, S., Brown, K., Islam, M. T., Hamm, L. L. and Nakhoul, N. L. (2015). Mechanisms of ammonia and ammonium transport by rhesus-associated glycoproteins. *Am. J. Physiol. Cell Physiol.* **309**, C747-C758.

Chasiotis, H., Ionescu, A., Misyura, L., Bui, P., Fazio, K., Wang, J., Patrick, M., Weihrauch, D. and Donini, A. (2016). An animal homolog of plant Mep/Amt transporters promotes ammonia excretion by the anal papillae of the disease vector mosquito, Aedes aegypti. *J. Exp. Biol.* **219**, 1346-1355.

Cragg, M. M., Balinsky, J. B. and Baldwin, E. (1961). A comparative study of nitrogen excretion in some amphibia and reptiles. *Comp. Biochem. Physiol.* **3**, 227-235.

Cruz, M. J., Sourial, M. M., Treberg, J. R., Fehsenfeld, S., Adlimoghaddam, A. and Weihrauch, D. (2013). Cutaneous nitrogen excretion in the African clawed frog Xenopus laevis: effects of high environmental ammonia (HEA). *Aquat Toxicol* **136-137**, 1-12.

Dames, P., Zimmermann, B., Schmidt, R., Rein, J., Voss, M., Schewe, B., Walz, B. and Baumann, O. (2006). cAMP regulates plasma membrane vacuolar-type H+-ATPase assembly and activity in blowfly salivary glands. *Proc. Natl. Acad. Sci. USA* **103**, 3926-3931.

Donini, A. and O'Donnell, M. J. (2005). Analysis of Na+, Cl-, K+, H+ and NH4+ concentration gradients adjacent to the surface of anal papillae of the mosquito Aedes aegypti: application of self-referencing ion-selective microelectrodes. *J. Exp. Biol.* **208**, 603-610.

Endeward, V., Cartron, J.-P., Ripoche, P. and Gros, G. (2008). RhAG protein of the Rhesus complex is a CO2 channel in the human red cell membrane. *FASEB J.* **22**, 64-73.

Ermak, T. H. and Eakin, R. M. (1976). Fine structure of the cerebral and pygidial ocelli in Chone ecaudata (Polychaeta: Sabellidae). *J. Ultrastruct. Res.* **54**, 243-260.

Evans, D. H., More, K. J. and Robbins, S. L. (1989). Modes of ammonia transport across the gill epithelium of the marine teleost fish Opsanus beta. *J. Exp. Biol.* **144**, 339-356.

Fanelli, G. M. and Goldstein, L. (1964). Ammonia excretion in the neotenous newt, *Necturus maculosus* (Rafinesque). *Comp. Biochem. Physiol.* **13**, 193-204.

Fehsenfeld, S. and Weihrauch, D. (2013). Differential acid-base regulation in various gills of the green crab *Carcinus maenas*: Effects of elevated environmental pCO2. *Comp. Biochem Physiol. A* **164**, 54-65.

Fehsenfeld, S. and Weihrauch, D. (2016). Mechanisms of acid–base regulation in seawater-acclimated green crabs (*Carcinus maenas*). *Can. J. Zool.* **94**, 95-107.

Fransen, M. E. (1988). Coelomic and vascular system. In *The ultrastructure of Polychaeta. Microfauna Marina*, Vol. 4, pp. 199-213.

Gardiner, S. L. (1988). Respiratory and feeding appendages. In. *The ultrastructure of Polychaeta. Microfauna Marina*, Vol. 4, pp. 37-43.

Gardiner, S. L. (1992). Polychaeta: General organization, integument, musculature, coelom and vascular system. In *Microscopic Anatomy of Invertebrates*, vol. 7, Annelida (ed. F. W. Harrisson and S. L. Gardiner), pp. 19–52. New York: Wiley-Liss.

Goldmann, R. and Rottenberg, H. (1973). Ion distribution in lysosomal suspensions. *FEBS Lett.* **33**, 233-238.

Harris, J. L., Maguire, G. B., Edwards, S. and Hindrum, S. M. (1998). Effect of ammonia on the growth rate and oxygen consumption of juvenile greenlip abalone, Haliotis laevigata Donovan. *Aquaculture* **160**, 259-272.

Hausen, H. (2005). Comparative structure of the epidermis in polychaetes (Annelida). *Hydrobiologia* **535**, 25-35.

Hu, M. Y., Lee, J.-R., Lin, L.-Y., Shih, T.-H., Stumpp, M., Lee, M.-F., Hwang, P.-P. and Tseng, Y.-C. (2013). Development in a naturally acidified environment: Na+/H+-exchanger 3-based proton secretion leads to CO2 tolerance in cephalopod embryos. *Front. Zool.* **10**, 51.

Kulkarni, G. K., Kulkarni, V. D. and Rao, A. B. (1989). Nephridial excretion of ammonia and urea in the freshwater leech, *Poecilobdella viridis* as a function of temperature and photoperiod. *Proc. Indian Natn. Sci. Acad.* **B55**, 345-352.

Kustu, S. and Inwood, W. (2006). Biological gas channels for NH3 and CO2: evidence that Rh (Rhesus) proteins are CO2 channels. *Transfus. Clin. Biol.* **13**, 103-110.

Larsen, E. H., Deaton, L. E., Onken, H., O'Donnell, M., Grosell, M., Dantzler, W. H. and Weihrauch, D. (2014). Osmoregulation and excretion. *Comp. Physiol.* **4**, 405-573.

Le Moullac, G. and Haffner, P. (2000). Environmental factors affecting immune responses in Crustacea. *Aquaculture* **191**, 121-131.

Ludewig, U., von Wirén, N. and Frommer, W. B. (2002). Uniport of NH4+ by the root hair plasma membrane ammonium transporter LeAMT1;1. *J. Biol. Chem.* **277**, 13548-13555.

Mangum, C. P., Dykens, J. A., Henry, R. P. and Polites, G. (1978). The excretion of NH4+ and its ouabain sensitivity in aquatic annelids and molluscs. *J. Exp. Zool.* **203**, 151-157.

Martin, M., Fehsenfeld, S., Sourial, M. M. and Weihrauch, D. (2011). Effects of high environmental ammonia on branchial ammonia excretion rates and tissue Rh-protein mRNA expression levels in seawater acclimated Dungeness crab Metacarcinus magister. *Comp. Biochem. Physiol. A Mol. Integr. Physiol.* **160**, 267-277.

Masui, D. C., Furriel, R. P. M., McNamara, J. C., Mantelatto, F. L. M. and Leone, F. A. (2002). Modulation by ammonium ions of gill microsomal (Na+,K+)-ATPase in the swimming crab Callinectes danae: a possible mechanism for regulation of ammonia excretion. *Comp. Biochem. Physiol. C Toxicol. Pharmacol.* **132**, 471-482.

Menendez, A., Arias, J. L., Tolivia, D. and Alvarez-Uria, M. (1984). Ultrastructure of gill epithelial cells of Diopatra neapolitana (Annelida, Polychaeta). *Zoomorphology* **104**, 304-309.

Nakada, T., Westhoff, C. M., Kato, A. and Hirose, S. (2007). Ammonia secretion from fish gill depends on a set of Rh glycoproteins. *FASEB J.* **21**, 1067-1074.

Nawata, C. M., Hirose, S., Nakada, T., Wood, C. M. and Kato, A. (2010). Rh glycoprotein expression is modulated in pufferfish (Takifugu rubripes) during high environmental ammonia exposure. *J. Exp. Biol.* **213**, 3150-3160.

O'Donnell, M. J. (1997). Mechanisms of excretion and ion transport in invertebrates. In *Comparative Physiology* (ed. W. H. Dantzler), pp. 1207-1289. New York: Oxford University Press.

Panz, M., Vitos-Faleato, J., Jendretzki, A., Heinisch, J. J., Paululat, A. and Meyer, H. (2012). A novel role for the non-catalytic intracellular domain of Neprilysins in muscle physiology. *Biol. Cell* **104**, 553-568.

Perry, S. F., Braun, M. H., Noland, M., Dawdy, J. and Walsh, P. J. (2010). Do zebrafish Rh proteins act as dual ammonia-CO2 channels? *J. Exp. Zool. A Ecol. Genet. Physiol.* **313**, 618-621.

Pitts, R. J., Derryberry, S. L., Jr, Pulous, F. E. and Zwiebel, L. J. (2014). Antennal-expressed ammonium transporters in the malaria vector mosquito Anopheles gambiae. *PLoS ONE* **9**, e111858.

Purschke, G., Bleidorn, C. and Struck, T. (2014). Systematics, evolution and phylogeny of Annelida–a morphological perspective. *Mem. Mus. Vic.* **71**, 247-269.

Purschke, G., Hugenschütt, M., Ohlmeyer, L., Meyer, H. and Weihrauch, D. (2016). Structural analysis of the branchiae and dorsal cirri in *Eurythoe complanata* (Annelida, Amphinomida). *Zoomorphology*, doi:10.1007/s00435-016-0336-5.

Quijada-Rodriguez, A. R., Treberg, J. R. and Weihrauch, D. (2015). Mechanism of ammonia excretion in the freshwater leech Nephelopsis obscura: characterization of a primitive Rh protein and effects of high environmental ammonia. *Am. J. Physiol. Regul. Integr. Comp. Physiol.* **309**, R692-R705.

Reitze, M. and Schöttler, U. (1989). The time dependence of adaption to reduced salinity in the lugworm Arenicola marina L. (Annelida: Polychaeta). *Comp Biochem. Physiol. Part A Physiol.* **93**, 549-559.

Riestenpatt, S., Onken, H. and Siebers, D. (1996). Active absorption of Na+ and Cl- across the gill epithelium of the shore crab Carcinus maenas: voltage-clamp and ion-flux studies. *J. Exp. Biol.* **199**, 1545-1554.

Rouse, G. W. and Pleijel, F. (2001). *Polychaetes*. New York: Oxford University Press, Oxford.

Smith, P. R. (1992). Excretory system. In *Microscopic Anatomy of Invertebrates*, vol. 7 Annelida (ed. F. W. Harrisson and S. L. Gardiner), pp. 71-108. New York: Wiley-Liss.

Soupene, E., Inwood, W. and Kustu, S. (2004). Lack of the Rhesus protein Rh1 impairs growth of the green alga Chlamydomonas reinhardtii at high CO2. *Proc. Natl. Acad. Sci. USA* **101**, 7787-7792.

Storch, V. and Alberti, G. (1978). Ultrastructural observations on the gills of polychaetes. *Helgoländ. Wiss. Meer.* **31**, 169-179.

Tillinghast, E. K. (1967). Excretory pathways of ammonia and urea in the earthworm Lumbricus terrestris L. *J. Exp. Zool.* **166**, 295-300.

Tillinghast, E. K., O'Donnell, R., Eves, D., Calvert, E. and Taylor, J. (2001). Water-soluble luminal contents of the gut of the earthworm Lumbricus terrestris L. and their physiological significance. *Comp. Biochem. Physiol. A Mol. Integr. Physiol.* **129**, 345-353.

Tresguerres, M., Parks, S. K., Salazar, E., Levin, L. R., Goss, G. G. and Buck, J. (2010). Bicarbonate-sensing soluble adenylyl cyclase is an essential sensor for acid/base homeostasis. *Proc. Natl. Acad. Sci. USA* **107**, 442-447.

Weihrauch, D. and O'Donnell, M. J. (2015). Links between osmoregulation and nitrogen-excretion in insects and crustaceans. *Integr. Comp. Biol.* **55**, 816-829.

Weihrauch, D., Becker, W., Postel, U., Riestenpatt, S. and Siebers, D. (1998). Active excretion of ammonia across the gills of the shore crab *Carcinus maenas* and its relation to osmoregulatory ion uptake. *J. Comp. Physiol. B* **168**, 364-376.

Weihrauch, D., Becker, W., Postel, U., Luck-Kopp, S. and Siebers, D. (1999). Potential of active excretion of ammonia in three different haline species of crabs. *J. Comp. Physiol. B* **169**, 25-37.

Weihrauch, D., Ziegler, A., Siebers, D. and Towle, D. W. (2002). Active ammonia excretion across the gills of the green shore crab *Carcinus maenas*: participation

of Na(+)/K(+)-ATPase, V-type H(+)-ATPase and functional microtubules. *J. Exp. Biol.* **205**, 2765-2775.
Weihrauch, D., Morris, S. and Towle, D. W. (2004). Ammonia excretion in aquatic and terrestrial crabs. *J. Exp. Biol.* **207**, 4491-4504.
Weihrauch, D., Wilkie, M. P. and Walsh, P. J. (2009). Ammonia and urea transporters in gills of fish and aquatic crustaceans. *J. Exp. Biol.* **212**, 1716-1730.
Weihrauch, D., Donini, A. and O'Donnell, M. J. (2011). Ammonia transport by terrestrial and aquatic insects. *J. Insect Physiol.* **58**, 473-487.
Weihrauch, D., Chan, A. C., Meyer, H., Doring, C., Sourial, M. M. and O'Donnell, M. J. (2012). Ammonia excretion in the freshwater planarian Schmidtea mediterranea. *J. Exp. Biol.* **215**, 3242-3253.
Weng, X.-H., Huss, M., Wieczorek, H. and Beyenbach, K. W. (2003). The V-type H(+)-ATPase in Malpighian tubules of Aedes aegypti: localization and activity. *J. Exp. Biol.* **206**, 2211-2219.
Westheide, W. (1997). The direction of evolution within the Polychaeta. *J. Nat. Hist.* **31**, 1-15.
Wood, C. M., Munger, R. S. and Toews, D. P. (1989). Ammonia, urea and H^+ distribution and the evolution of ureotelism in amphibians. *J. Exp. Biol.* **144**, 215-233.
Wright, P. A. (1995). Nitrogen excretion: three end products, many physiological roles. *J. Exp. Biol.* **198**, 273-281.
Wright, P. A. and Wood, C. M. (2009). A new paradigm for ammonia excretion in aquatic animals: role of Rhesus (Rh) glycoproteins. *J. Exp. Biol.* **212**, 2303-2312.
Young-Lai, W. W., Charmantier-Daures, M. and Charmantier, G. (1991). Effect of ammonia on survival and osmoregulation in different life stages of the lobster Homarus americanus. *Mar. Biol.* **205**, 293-300.